http://dx.doi.org/10.5012/bkcs.2014.35.12.3576

Electrochemical Behavior of Pt-Ru Catalysts on Zeolite-templated Carbon Supports for Direct Methanol Fuel Cells

Tae-Jin Lim, Seul-Yi Lee, Yoon-Jong Yoo,† and Soo-Jin Park*

*Department of Chemistry, Inha University, Incheon 402-751, Korea. *E-mail: sjpark@inha.ac.kr*
†Reaction and Separation Materials Research Center, Korea Institutes of Energy Research, Daejeon 305-343, Korea
Received April 15, 2014, Accepted August 25, 2014

Zeolite-templated carbons (ZTCs), which have high specific surface area, were prepared by a conventional templating method using microporous zeolite-Y for catalyst supports in direct methanol fuel cells. The ZTCs were synthesized at different temperatures to investigate the characteristics of the surface produced and their electrochemical properties. Thereafter, Pt-Ru was deposited at different carbonization temperatures by a chemical reduction method. The crystalline and structural features were investigated using X-ray diffraction and scanning electron microscopy. The textural properties of the ZTCs were investigated by analyzing N_2/77 K adsorption isotherms using the Brunauer-Emmett-Teller equation, while the micro- and meso-pore size distributions were analyzed using the Barrett-Joyner-Halenda and Harvarth-Kawazoe methods, respectively. The surface morphology was characterized using transmission electron microscopy and inductively coupled plasma-mass spectrometry. The electrochemical properties of the Pt-Ru/ZTCs catalysts were also analyzed by cyclic voltammetry measurements. From the results, the ZTCs carbonized at 900 °C show the highest specific surface areas. In addition, ZTC900-PR led to uniform dispersion of Pt-Ru on the ZTCs, which enhanced the electro-catalytic activity of the Pt-Ru catalysts. The particle size of ZTC900-PR catalyst is about 3.4 nm, also peak current density from the CV plot is 12.5 mA/cm^2. Therefore, electro-catalytic activity of the ZTC900-PR catalyst is higher than those of ZTC1000-PR catalyst.

Key Words : Microporous carbon, Pt-Ru catalysts, Electro-catalytic properties, Zeolite-templated carbon

Introduction

Currently, owing to the problems associated with the exhaustion of fossil fuels, global warming, *etc*., studies on hydrogen as an energy carrier have been conducted globally, including in Korea. Moreover, the goal of various hydrogen project fields, including fuel cells, is to develop a system for generating and storing hydrogen; for this purpose, various hydrogen-storage materials and systems have been researched and developed.[1]

Fuel cells are generator units transforming the energy generated during the oxidation of hydrogen into electric energy. They are gaining importance because they use hydrogen as the energy source; moreover, they are clean and show far higher electric efficiency than other generator units.[2,3] Moreover, fuel cells are one of the most convenient energy sources at present where portable electronic products such as mobile phones and laptops have gained popularity among ordinary people owing to the rapid development of the modern electronics industry. Although portable electronic products are popular, the batteries used as power supplies for such products have not yet delivered satisfactory performance. Moreover, these batteries are expensive. To fulfill such demand, development attempts and studies on direct methanol fuel dells (DMFCs), which can be miniaturized and can use methanol as fuel, have been conducted.[4] Although several studies are being currently conducted because of the advantages of low operating temperature, ease of handling, high energy density of the methanol fuel, and convenience of directly supplying the fuel, the oxidation of methanol is a considerably complex reaction and proceeds at a very low rate; thus, the acceleration of the electrochemical reaction is necessary. The electrode of a DMFC consists of a support layer and a catalyst layer; Pt is mainly used for the catalyst.[5] In a DMFC, methanol produces hydrogen ions through the catalyst, which is required to operate safely and have excellent catalytic activity; thus, studies in this regard have only been directed at using Pt because this metal satisfies these requirements. However, several problems are associated with the use of Pt. Pt catalysts are not competitive with regard to cost, and their activities are weak because they strongly compete with carbon monoxide, and thus the surface becomes toxic.[6-9]

To solve such problems, studies are being conducted to develop a reformer that can completely eliminate CO in the production step; these reformers can include bimetallic or trimetallic catalysts containing platinum, as well as non-Pt-electrode catalysts.[10-13] Of these attempts, one of the simplest ways to minimize the poisoning effect of CO and improve the performance of the electrode catalyst is to produce a bimetallic alloy catalyst by adding a second element to the platinum. Of the various kinds of bimetallic catalysts used to increase the CO tolerance of DMFC anodes, Pt–Ru is commonly used at present. Here, Ru dissociates water and produces OH^-, which oxidizes CO to CO_2, and thus is frequently employed.

Moreover, studies have been conducted on catalyst supports that can reduce the use of platinum and enhance safety by increasing their usability after evenly dispersing the catalyst to reduce the required catalyst amount. Additionally, carbon materials, which have excellent chemical stabilities, high electric conductivities, and high specific areas, are mainly used. For example, methods for depositing Pt–Ru on carbon nanotubes (CNTs) are being studied to enable the use of the latter as catalyst supports, and even a small amount of Pt–Ru can improve their voltage and power density.[12]

According to the thesis of Ruhit Jyoti Konwar, zeolite templated-carbon (ZTC) is a type of microporous carbon with high specific surface area.[13,14] Many researchers have predicted that carbon in ZTCs can be potentially used for hydrogen storage; moreover, the use of ZTCs as supports for platinum catalysts in electric double-layer capacitors and DMFCs has been studied in various research fields, and several studies on the physiochemical properties and potential applications of ZTCs have been conducted.[15,16] ZTC is used as a support for platinum catalysts, and is a suitable candidate for an electric catalyst because it has high specific surface area.[17]

Thus, in the present study, we synthesized carbon materials by the template synthesis method using zeolite-Y, and used them as catalyst supports. The synthesized microporous carbon is called ZTC. The high specific surface area of ZTC provides a condition for improving the electric performance of the metal-carbon support catalyst. After manufacturing a bimetallic catalyst (Pt–Ru/C), in which various proportions of Pt and Ru were deposited using ZTC, we analyzed the activity and characteristics of the catalyst.[15-18]

Experimental

Synthesis of Microporous Carbon. Microporous carbons were synthesized by using microporous zeolite-Y powders (CBV721, Zeolyst International) as templates and furfuryl alcohol ($C_5H_6O_2$, Sigma Aldrich). We obtained microporous carbon through a heat-treatment process and after removing zeolite-Y after filling the microporous zeolite-Y powder with furfuryl alcohol, which is a carbon precursor. We stirred a mixture of 20 mL of furfuryl alcohol and 5 g of zeolite-Y at room temperature for more than 5 days to combine them. Then, we washed and filtered them with mesitylene (C_9H_{12}, Sigma Aldrich), and dried them in a vacuum oven at 353 K for 24 h. After this process, we stabilized them in a nitrogen atmosphere at 423 K for 8 h, and carbonized them at 1023, 1123, 1173, and 1273 K for 4 h. During the carbonizing process, the heating rate was set to 2 °C/min. We removed the zeolite of the carbonized sample by using 5 wt % of hydrofluoric acid (HF, 35%, DUKSAN). Then, we conducted additional cleaning and filtering using distilled water and ethanol, and conducted complete drying in an oven at 353 K for 24 h.[18,19]

Preparation of Pt-Ru Catalyst. For catalyst deposition, a reducing agent was used according to the literature.[21-25] Firstly, 0.3 g of carbon support (ZTC) was mixed with 150 mL of ethylene glycol ($C_2H_4OH_2$, 99 wt %, Sigma Aldrich) solution or distilled water, and it was dispersed using ultrasonication for 30 min. To deposit the support with 30 wt % of Pt-Ru, the ethylene glycol solution, mixed with 0.237 g of chloroplatinic acid (H_2PtCl_6, Sigma Aldrich) and 0.186 g of ruthenium chloride ($RuCl_3$, Sigma Aldrich, the Ru precursor), was slowly introduced into the carbon dispersion solution and stirred for 5 h. To control the pH of the mixed solution, 50 mL of 0.1-M sodium hydroxide was added, and the solution was maintained at 410 K for 3 h. All the manufacturing processes were conducted in a nitrogen (N_2) atmosphere. We obtained the catalyst after filtering the solid powder, washing it with distilled water, and drying it at 340 K for 24 h.

Characterization. To characterize the synthesized carbon support and the change in its microstructure, we used X-ray diffraction spectroscopy (XRD; Rigaku Model D/Max), and we determined the surface and morphological features using a scanning electron microscope (SEM; Hitachi S-4300). The synthesized carbon support, specific surface area, and isothermal absorption curve of the catalyst were measured at 77 K using a surface area and pore-size analyzer (Bersorp, Japan, Inc.). For the synthesized carbon support and specific surface area of the catalyst (S_{BET}), we used the Brunauer–Emmett–Teller (BET) equation, and the total pore volume (V_{Total}) was obtained from the amount of the nitrogen absorbed for the condition $P/P_0 = 0.990$. A transmission electron microscope (TEM; JEM 2100F) was used to examine the particle size of the electrode catalyst for the synthesized DMFCs and the distribution of the Pt-Ru. Moreover, to measure the amount of Pt-Ru deposition, we conducted a quantitative analysis using a plasma-mass spectrometer (ICP-MS; ELAN 6100).

To measure the cyclic voltammetry (CV) curve corresponding to the case of the Pt-Ru catalyst deposited on the carbon support, we used Autolab with PGSTAT 30 (Eco Chemie B. V.; Netherlands) as the electrochemical measurement apparatus. We attached a certain amount of catalyst to the working electrode using carbon paste, and used Ag/AgCl as the standard electrode and Pt wire as the counter electrode. For the measurement electrode, we used a solution of 0.5-M H_2SO_4 and 1-M of MeOH. The electric potential scan rate was fixed at 20 mV/s.

Results and Discussion

Characterization of Microporous Carbon. To examine the structural features of zeolite-Y and the synthesized ZTC microporous carbon supports, we used an X-ray diffractometer, and the results are shown in Figure 1.

As can be seen in Figure 1, we identified a peak of zeolite at an angle of 6°, and the highest and sharpest peak was attributed to the (111) plane. Furthermore, we also checked for peaks of the ZTC, which was a carbon support used to carbonate FA-deposited zeolite treated at 750 °C, 850 °C, 900 °C, and 1000 °C, and FA did not have any large influence on the zeolite, but unlike the peak for zeolite, the peak of ZTC was confirmed to be offset. It appears that the peak was

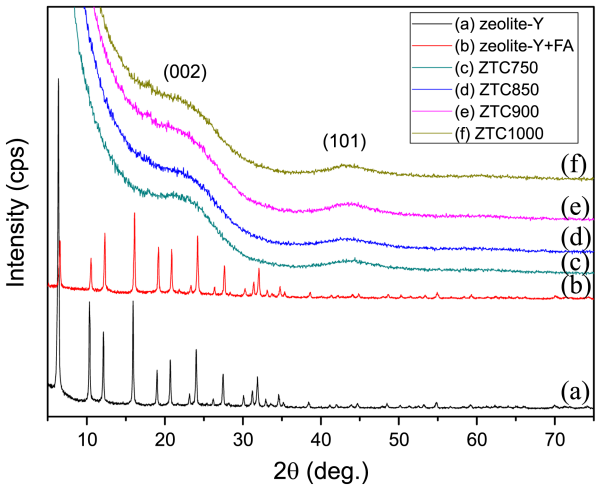

Figure 1. High-angle XRD curves of zeolite-Y, zeolite-Y+FA, and ZTCs.

offset because of HF and thermal treatments. The fine-carbon characteristic peaks of ZTC, which correspond to the (002) and (101) planes at 26° and 44°, respectively. By inspection of these, it was deemed that the carbon structure was deformed, and the 26° and 44° peaks disappeared as the crystal structure in the carbon collapsed with change in the temperature of the thermal treatment.[26]

Figure 2 shows the SEM images of ZTCs treated at different temperatures. As can be seen in the SEM results, the surface and structural deformation states of ZTCs treated at various temperatures showed inconsistencies such as irregular surfaces and arrangement states. Moreover, when the temperature of carbonizion increased, the structures collapsed, and a structural deformation similar to that of an amorphous form of ZTC occurred.

Through the nitrogen adsorption–desorption experiment with ZTC, we obtained the specific surface area, respective mean volumes of mesopores and micropores, and overall pore volume and average pore size. The results are shown in Table 1. The average pore size was obtained using the

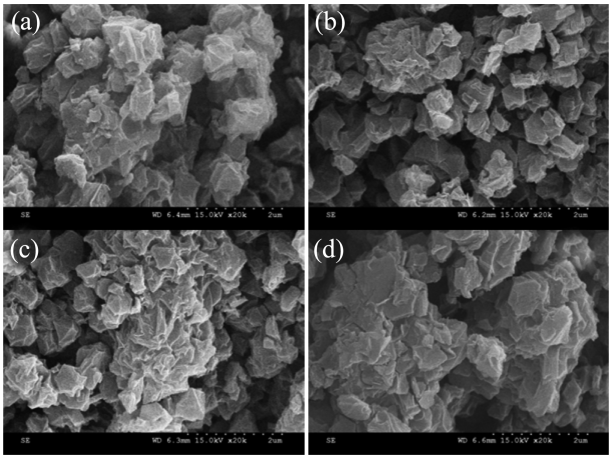

Figure 2. SEM images of ZTCs: (a) ZTC750; (b) ZTC850; (c) ZTC900; (d) ZTC1000.

Table 1. Textural Properties of ZTCs

Samples	S_{BET}[a] (m^2/g)	V_{Total}[b] (cm^3/g)	V_{Micro}[c] (cm^3/g)	V_{Meso}[d] (cm^3/g)	D_P[e] (nm)
ZTC750	1380	1.02	0.44	0.58	2.97
ZTC850	1550	1.14	0.52	0.62	3.00
ZTC900	1710	1.32	0.55	0.77	3.07
ZTC1000	1620	1.30	0.49	0.81	3.22

[a]S_{BET}: Specific surface area calculated using the Brunauer-Emmett-Teller equation at a relative pressure range 0.03–0.22. [b]V_{Total}: Total pore volume estimated at a relative pressure $P/P_0 = 0.990$. [c]V_{Micro}: Micropore volume determined from the subtraction of mesopore volume from total pore volume. [d]V_{Meso}: Mesopore volume determined from the Barret-Joyner-Halenda (BJH) equation. [e]D_P: Average pore diameter.

following formula.[21,27]

$$D(\text{nm}) = \frac{4V_{Total} \times 1000}{S_{SET}} \quad (1)$$

As can be seen in Table 1, the entire specific surface area and entire pore volume, as well as the mesopore, micropore, and average pore volumes, tend to increase. However, when the micropores were carbonized at 900 °C, the average micropore size increased by 0.55 cm^3/g, whereas when the ZTC was carbonized at 1000 °C, the specific surface area decreased; the average micropore size also decreased by 0.49 cm^3/g. Converting this value to pore volume, the void content at a carbonization temperature of 900 °C was the highest by 42%, whereas the micropore content for a carbonization temperature of 1000 °C largely decreased by 37%. The pore specific surface area increased and the micropore size decreased after the high-temperature thermal treatment, corresponding to the results of previous X-ray diffraction analysis. This was because when the thermal treatment temperature increased, the micropore size in the carbon continued to increase, leading to the collapse of the inner side.[27]

Figure 3 is a graph of the results of calculating the pore size from the nitrogen adsorption–desorption isotherm curve generated using the BET method.

In Figure 3, ZTC900 represents the Type IV Langmuir

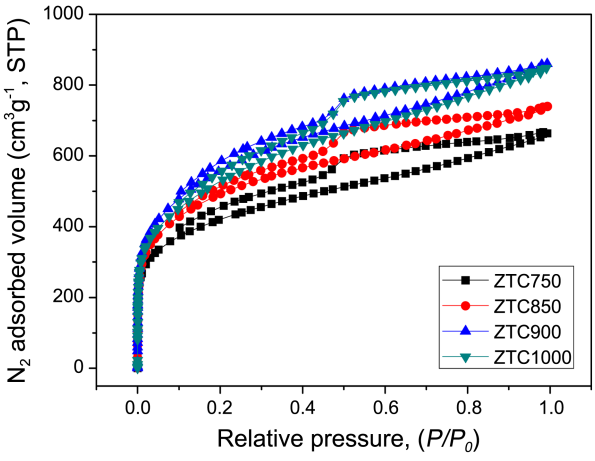

Figure 3. Nitrogen adsorption-desorption isotherms of ZTCs.

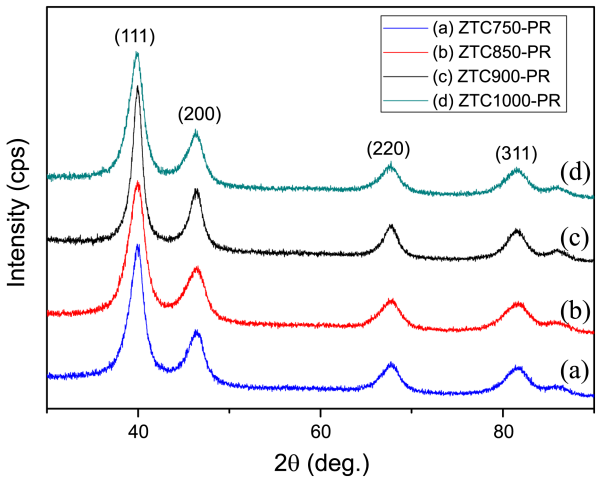

Figure 4. High-angle XRD curves of Pt-Ru catalysts.

nitrogen adsorption curve where micropores are developed. Here, N_2 adsorption increases when the pressure increases, and it shows constant adsorption above a certain pressure.[28]

The gradient of the adsorption–desorption isotherm curve of ZTC900 is more consistent than that of ZTC1000 because the total pore size and total micropore size decrease, while the mean mesopore size increases (Table 1). Furthermore, mesopores and smaller micropores are generated when thermal treatment of the carbon support is carried out at various temperatures. It appears that in the support material of ZTC1000, micropores were increasingly generated, and the average pores ultimately increased because the inner side of the support collapsed; at the same time, mesopores increased while the specific surface area and entire pore volume gradually decreased.

Characterization of Pt-Ru Catalysts. Figure 4 shows the XRD results of deposited Pt and Ru on different carbon supports treated at various temperatures. When we examine the XRD peaks, peaks of (111), (200), (220), and (311) surfaces of Pt-Ru are observed near 40°, 46°, 67°, and 82°, respectively, and it may be confirmed that the Pt-Ru was deposited onto the carbon support. By monitoring the intensity of the peaks, we confirm that there is no other difference, because the same amount of Pt-Ru was deposited. Regarding the crystal size of Pt-Ru, we were able to measure the average particle size by applying the Sherrer formula on the (220) plane located near $2\theta = 67°$.[29-31]

$$d = \frac{(K \cdot \lambda)}{\mathrm{FWHM} \cdot \cos\theta}. \quad (2)$$

Here, d is the diameter of the Pt-Ru particle; K is a constant that usually takes a value of 0.9; λ is the wavelength (Cu $K\alpha$, 0.1542 nm) of the X-ray; and FWHM and θ represent the full width at half maximum of the diffraction peak and the Bragg angle, respectively.

Table 2 shows the result of calculating the average particle size of Pt-Ru by using the Sherrer formula (2), and we confirmed that ZTC900-PR had the smallest size. Moreover, to confirm the deposition amount of Pt-Ru on the catalyst,

Table 2. Loading Contents and Mean Size of Pt-Ru Catalysts

Samples	Pt (wt %)[a]	Ru (wt %)[a]	Loading Level (%)[a]	Crystalline size (nm)[b]	Crystalline size (nm)[c]
ZTC750-PR	18.4	5.5	39.9	4.1 ± 0.2	4.0 ± 0.2
ZTC850-PR	19.0	6.3	42.2	3.8 ± 0.1	3.7 ± 0.1
ZTC900-PR	20.2	8.1	47.2	3.4 ± 0.1	3.3 ± 0.1
ZTC1000-PR	17.6	5.1	37.8	4.3 ± 0.1	3.9 ± 0.2

[a]Measured from ICP-MS results. [b]Measured from TEM results. [c]Measured from XRD results.

we display the results of the quantitative analysis obtained using ICP-MS in Table 2. The yield rate of the actual metal was determined by the loading level on the carbon support, and this refers to the ratio of the actual amount of metal deposited to the theoretically deposited amount on the carbon support. When comparing the deposition amounts of Pt-Ru, the ZTC900-PR catalyst showed the highest deposition rate and loading level. From Tables 1 and 2, it appears that Pt-Ru was highly dispersed with a stable mean size due to the high specific surface area and the fraction of the micropores of ZTC900, which was the carbon support.[24,25,32]

Table 3 shows the results of the nitrogen adsorption-desorption experiment with the catalyst where the Pt-Ru was deposited onto the carbon support at different temperatures. As can be seen in Tables 1 and 3, ZTC900, which is a carbon support, has a high specific surface area of 1700 (cm^2/g). When Pt-Ru is deposited onto the ZTC, the specific surface area decreases, and the pore size gradually decreases as the deposition amount increases, and this tendency could be confirmed by inspection of the nitrogen adsorption-desorption curve in Figure 5.

The probable reason why the specific surface area decreases as Pt-Ru is deposited onto the ZTC is that when Pt-Ru is deposited on the ZTC, it fills the pores. Moreover, the reason why the nitrogen adsorption-desorption curve of ZTC1000-PR assumes maximum values, despite the same amount of Pt-Ru being deposited, is because, the micropore fraction is reduced, whereas the mesopore size is the largest, and this reduces the deposition rate of the metal particles (Tables 1 and 2).

Figure 6 is a TEM image of four Pt-Ru-deposited ZTCs.[33] It can be confirmed that the ZTC750-PR, ZTC850-PR,

Table 3. Textural Properties of ZTC-PRs

Samples	S_{BET}[a] (m^2/g)	V_{Total}[b] (cm^3/g)	V_{Micro}[c] (cm^3/g)	V_{Meso}[d] (cm^3/g)	D_P[e] (nm)
ZTC750-PR	795	0.52	0.27	0.25	2.63
ZTC850-PR	1060	0.71	0.36	0.35	2.70
ZTC900-PR	925	0.61	0.31	0.30	2.67
ZTC1000-PR	1080	0.77	0.35	0.42	2.88

[a]S_{BET}: Specific surface area calculated using the Brunauer-Emmett-Teller equation at a relative pressure range of 0.03-0.22. [b]V_{Total}: Total pore volume estimated at a relative pressure $P/P_0 = 0.990$. [c]V_{Micro}: Micropore volume determined from the subtraction of mesopore volume from total pore volume. [d]V_{Meso}: Mesopore volume determined from the Barret-Joyner-Halenda (BJH) equation. [e]D_P: Average pore diameter.

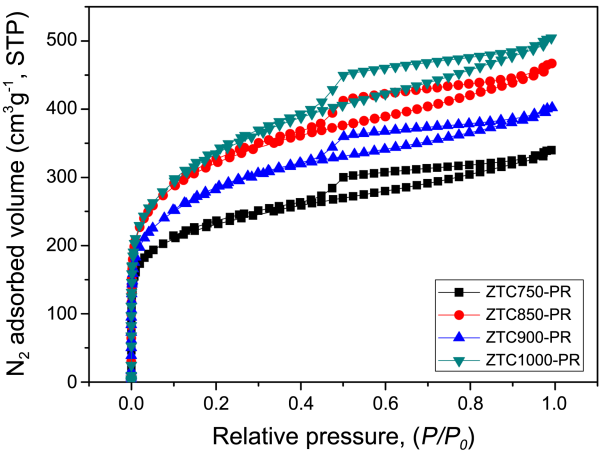

Figure 5. Nitrogen adsorption-desorption isotherms of ZTC-PRs.

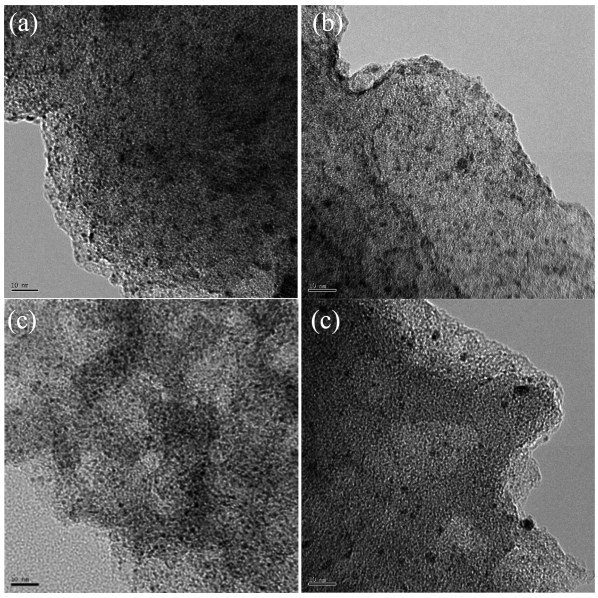

Figure 6. TEM images of (a) ZTC750-PR; (b) ZTC850-PR; (c) ZTC900-PR; (d) ZTC1000-PR.

ZTC900-PR, and ZTC1000-PR catalysts were dispersed; in particular, ZTC900-PR was well dispersed and the most homogeneous. Moreover, we measured the average metal particle sizes obtained from the TEM images and compared it with those obtained from the XRD analysis results. As can be seen in Table 2, we obtained the same result showing that the micropore fraction in ZTC1000-PR was larger than that for ZTC900. When the average size of the Pt-Ru metal particles in the carbon support is smaller, the dispersion is deemed to be more homogeneous. Accordingly, the pore blockage in the carbon support and the agglomeration of metal particles decrease, achieving a denser grid array. Ultimately, this leads to the enhancement of electrochemical properties.[24,25]

Electrochemical Features of Catalyst Electrode. CV is used for analyzing the interaction between metal and oxygen and also for determining electrochemical stability. We analyzed the oxidation-reduction reaction characteristics of the catalyst synthesized in a 0.5-M H_2SO_4 solution using CV

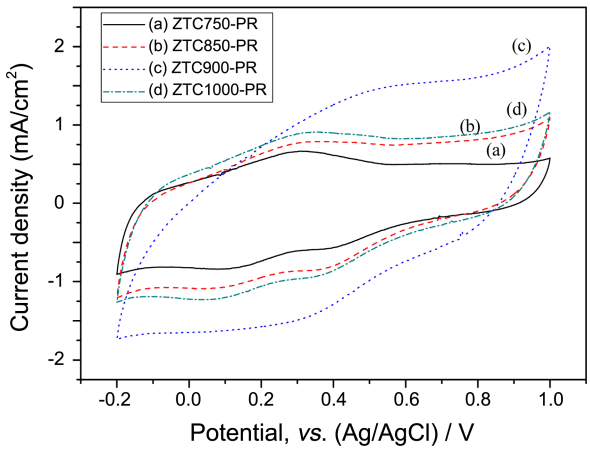

Figure 7. Cyclic voltammetry of Pt-Ru catalysts in 0.5-M H_2SO_4 at 20 mV/s of scan rate.

at a scanning speed of 20 mV/s and varying from −0.2 to 1.0 V (*vs*. Ag/AgCl).[34-37]

Figure 7 shows the voltammetry curve of the Pt–Ru catalyst using carbon supports carbonized at different temperatures. According to the Pt–Ru deposited voltammetry curves in Figure 7, it can be confirmed that the curve for the ZTC900-PR catalyst was far wider and larger than those for the catalyst deposited on other carbon supports. It appears that ZTC900 exhibits a higher current density than other supports because, as can be seen in Table 1, both the fraction of the specific surface area and the micropore size is considerably higher than those of other supports. For this reason, the dispersion of the Pt-Ru metal appears to be considerably higher than that for other carbon supports.[38]

Figure 8 shows the voltammetry curve for the activity of the Pt-Ru catalyst in solution, where 1-M CH_3OH and 0.5-M H_2SO_4 of the carbon supports carbonized at different temperatures. As can be seen in Figure 8, the oxidation reaction peak is large and clear in the region between 0.4 and 0.7 V. Moreover, the area near A is the peak demonstrating that the oxidation of methanol occurred. When the Pt-Ru metal was deposited onto the carbon supports treated at different

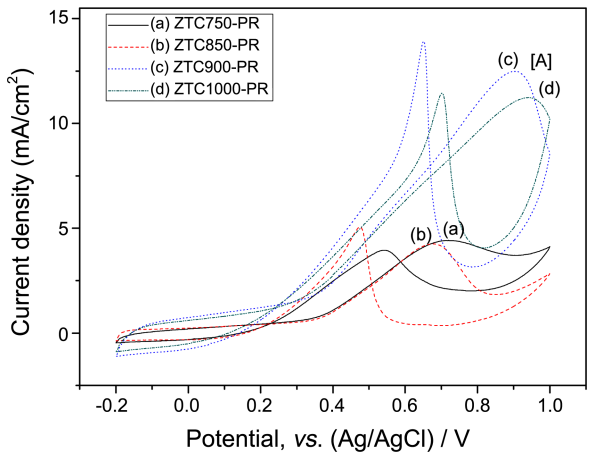

Figure 8. Cyclic voltammetry of Pt-Ru catalysts in 0.5-M H_2SO_4 + 1-M CH_3OH with 20 mV/s of scan rate.

temperatures, when manufacturing the ZTC, the change in the areas of A was confirmed as the temperature increased to 750, 850, 900, and 1000 °C. Many researchers have been focused on the methanol oxidation with Pt-Ru electro-catalysts.[39-41] The potential for methanol electro-oxidation, at which the peak current occurs, is 0.9 V and the peak current density is 12.5 mA/cm^2 during positive potential scanning on the Pt-Ru catalyst from the curve (c). The peak potential and the peak current density on the Pt-Ru catalyst are about 0.67 V and 14 mA/cm^2, respectively, during its reverse scanning. The peak potential for methanol electro-oxidation and the peak current density on the ZTC1000-PR catalyst are about 0.93 V and 11.0 mA/cm^2, respectively, during positive potential scanning as shown by curve (b). The peak potential and the peak current density on the ZTC1000-PR catalyst are about 0.7 V and 11.5 mA/cm^2, respectively, during its reverse scanning. The peak potential on the ZTC900-PR catalyst during potential scanning is 30 mV lower than that for the ZTC100-PR catalyst. But the peak current density for the ZTC900-PR catalyst is 1.5 mA/cm^2 higher than that for the ZTC1000-PR catalyst. So, the performance of ZTC900-PR catalyst for methanol electro-oxidation is much better than that for the ZTC-PRs catalyst.[42,43]

Meanwhile, it was found that the peak current density on the carbon black support (Vulcan XC-72 as a commercialized carbon support) deposited with Pt-Ru was about 7.4 mA/cm^2.[42,43] Compared to this results of carbon black support, the electro-catalytic activity of the ZTC900-PR catalyst is clearly improved, suggesting the promising Pt-Ru catalyst for DMFCs.

Conclusion

We synthesized ZTCs with high specific area through carbonation at various temperatures by a conventional templating method using zeolite-Y. Then, we used the ZTCs as the catalyst support for depositing the Pt–Ru metal catalyst for DMFCs to examine how it affects the electrochemical characteristics. We confirmed that the electrochemical characteristics of the ZTC900-PR catalyst, where the Pt-Ru catalyst was deposited on ZTC900 carbonized at 900 °C, was the most excellent. Moreover, as is evident from the results of cyclic voltammetry, the ZTC900-PR catalyst, which was produced through carbonization at temperatures 50 °C higher than that of the ZTC850-PR catalyst, which was deposited on the ZTC850 carbon support carbonized at 850 °C, showed 1.5 times better electrochemical performance. However, the ZTC1000-PR catalyst, where Pt-Ru was deposited onto the ZTC1000 carbonized at temperatures 100 °C higher, showed poorer electrochemical characteristics than the ZTC900-PR catalyst. While the size of the Pt-Ru particles deposited onto ZTC900-PR was 3.4–3.5 nm, those of the Pt-Ru particles deposited onto ZTC1000-PR were in the range 4.3–4.4 nm. Thus, because aggregation of the particles occurred, the specific surface area and pore size greatly decreased. Accordingly, the Pt-Ru metal catalyst could not enhance the electrochemical characteristics any further. In conclusion, in the manufacture of the microporous ZTC, the optimal temperature, at which the maximum electrochemical activity of the Pt-Ru deposited catalyst occurs, is 900 °C. However, when deposition is conducted at temperatures higher than 900 °C, the electrochemical performance deteriorates owing to catalyst dispersion and structural combination of the carbon supports.

Acknowledgments. This work was supported by Korea Ministry of Environment (MOE) as "GAIA Program" and KIER Core Research Program and the Carbon Valley Project of the Ministry of Knowledge Economy, Korea.

References

1. Cropper, M. A. J.; Geiger, S.; Jollie, D. M. *J. Power Sources* **2004**, *131*, 57.
2. Ilic, D.; Holl, K.; Brike, P.; Wohrle, T.; Brike-Salam, F. *J. Power Sources* **2006**, *155*, 1.
3. Kim, S.; Park, S. J. *Electrochim. Acta* **2007**, *52*, 3013.
4. Kawaguchi, T.; Sugiimoto, W.; Murakami, Y.; Takasu, Y. *J. Catal.* **2005**, *229*, 176.
5. Kim, B. J.; Park, S. J. *Polym-Korea* **2011**, *22*, 2.
6. Jung, S. M.; Shin, J. K.; Kim, K. S.; Baek, S. H.; Tak, Y. S. *Appl. Chem. Eng.* **2010**, *21*, 537.
7. Nitani, H.; Nakagawa, T.; Daimon, H.; Kurobe, Y.; Ono, T.; Honda, Y.; Koizumi, A.; Seino, S.; Yamamoto, T. A. *Appl. Catal., A* **2007**, *326*, 2.
8. Li, X.; Chen, W. X.; Zhao, J.; Xing, W.; Xu, Z. *Carbon* **2005**, *43*, 2168.
9. Nam, K. D.; Kim, T. J.; Kim, S. K.; Lee, B. R.; Peck, D. H.; Ryu, S. K.; Jung, D. H. *Korean J. Chem. Eng.* **2006**, *17*, 223.
10. Xu, J. B.; Zhao, T. S.; Liang, Z. X. *J. Power Sources* **2008**, *185*, 857.
11. Choi, S. M.; Seo, M. H.; Kim, H. J.; Lim, E. J.; Kim, W. B. *Int. J. Hydrogen Energ.* **2010**, *35*, 6853.
12. Park, S. J.; Park, B. J.; Ryu, S. K. *Carbon* **1999**, *37*, 1223.
13. Youn, H. K.; Kim, J.; Chandrasekar, G.; Jin, H.; Ahn, W. S. *Mater. Lett.* **2011**, *65*, 1772.
14. Konwar, R. J.; De, M. *Microporous Mesoporous Mater.* **2013**, *175*, 16.
15. Su, F. N.; Zeng, H. J.; Yu, Y.; Lv, J.; L.; Lee, J. Y.; Zhao, X. S. *Carbon* **2005**, *43*, 2368.
16. Coker, E. N.; Steen, W. A.; Miller, J. T.; Kropf, A. J.; Miller, J. E. *J. Mater Chem.* **2007**, *17*, 3330.
17. Coker, E. N.; Steen, W. A.; Miller, J. E. *Microporous Mesoporous Mater.* **2007**, *104*, 236.
18. Zhao, D.; Feng, J.; Huo, Q.; Melosh, N.; Fredirckson, G. H.; Chemlka, B. F.; Stucky, G. D. *Science* **1998**, *279*, 548.
19. Sakamoto, Y.; Kaneda, M.; Terasaki, O.; Zhao, D. Y.; Kim, J. M.; Stucky, G.; Shin, H. J.; Ryoo, R. *Nature* **2000**, *408*, 449.
20. Nishihara, H.; Hou, P. X.; Li, L. X.; Ito, M.; Uchiyama, M.; Kaburagi, T.; Ikura, A.; Katamura, J.; Kawarada, T.; Mizuuchi, K.; Kyotani, T. *J. Phys. Chem.* **2009**, *113*, 3189.
21. Kim, S.; Lee, J. R.; Park, S. J. *Korean Chem. Eng. Res*. **2008**, *46*, 118.
22. Kim, S.; Park, S. J. J. *Solid State Electrochem.* **2007**, *11*, 821.
23. Kim, D. S.; Guiver, M. D.; Yun, T. I.; S, M. Y.; Rhim, J. W. *J. Solid State Electrochem.* **2006**, *281*, 156.
24. Tokarz, W.; Lota, G.; Fackowiak, E.; Czerwiński, A.; Piela, P. *Electrochim Acta* **2013**, *98*, 95.
25. Lee, S. Y.; Kim, B. J.; Park, S. J. *Energy* **2014**, *66*, 72.
26. Park, S. J.; Seo, M. K.; Lee, Y. S. *Carbon* **2003**, *41*, 723.
27. Kim, Y. H.; Park, S. J. *Appl. Chem. Eng.* **2010**, *21*, 183.

28. Im, J. S.; Park, S. J.; Lee, Y. S. *J. Colloid Interface Sci.* **2007**, *314*, 32.
29. Han, D. M.; Guo, Z. P.; Zhao, Z. W.; Zeng, R.; Meng, Y. Z.; Shu, D.; Liu, H. K. *J. Power Sources* **2008**, *184*, 361.
30. Jeyabharathi, C.; Mathiyarasu, J.; Phani, K. L. N. *J. Appl. Electrochem.* **2009**, *39*, 45.
31. Prabhuram, J.; Zhao, T. S.; Wong, C. W.; Guo, J. W. *J. Power Sources* **2004**, *134*, 1.
32. Seredych, M.; Hulicova-Jurcakova, D.; Lu, G. Q.; Bandosz, T. J. *Carbon* **2008**, *46*, 1475.
33. Kunz, H. R.; Gruver, G. A. *J. Electrochem. Soc.* **1975**, *122*, 1279.
34. Tang, S.; Vongehr, S.; He, G.; Chen, L.; Meng, X. *J. Colloid Interface Sci.* **2012**, *125*, 375.
35. Kim, S. K.; Park, J. Y.; Hwang, S. C.; Lee, D. K.; Lee, S. H.; Rhee, Y. W.; Han, M. H. *J. Clean Technology* **2013**, *19*, 320.
36. Woo, J. Y.; Lee, K. M.; Jee, B. C.; Ryu, C. H.; Yoon, C. H.; Chung, J. H.; Kim, Y. R.; Moon, S. B.; Kang, A. S. *J. Ind. Eng. Chem.* **2010**, *16*, 688.
37. Lo, A. Y.; Hung, C. T.; Yu, N.; Kuo, C. T.; Liu, S. B. *Appl Energ* **2012**, *100*, 66.
38. Lee, S. Y.; Kim, B. J.; Park, S. J. *J. Solid State Chem.* **2013**, *199*, 258.
39. Prado-Burguete, C.; Linares-Solano, A.; Rodríguez-Reinoso, F.; Salinas-Martínez, C. *J. Catal.* **1989**, *115*, 98.
40. Zainoodin, A. M.; Kamarudin, S. K.; Daud, W. R. W. *Int. J. Hydrogen Eng.* **2010**, *35*, 4604.
41. Hsieh, C. T.; Lin, J. Y. *J. Power Sources* **2009**, *188*, 347.
42. Wang, Z. B.; Yin, G. P.; Zhang, J.; Sun, Y. C.; Shi, P. F. *Electrochemica Acta* **2006**, *51*, 5695.
43. Kim, S.; Park, S. J. *J. Power Sources* **2006**, *159*, 42.